Am. J. Hum. Genet. 70:955–964, 2002

Newfoundland Rod-Cone Dystrophy, an Early-Onset Retinal Dystrophy, Is Caused by Splice-Junction Mutations in *RLBP1*

Erica R. Eichers,[1,*] Jane S. Green,[5,6,7,*] David W. Stockton,[1,3,4] Christopher S. Jackman,[7,8] James Whelan,[5] J. Arch McNamara,[5,9] Gordon J. Johnson,[5,10] James R. Lupski,[1,2,4] and Nicholas Katsanis[1,11]

Departments of [1]Molecular and Human Genetics, [2]Pediatrics, and [3]Medicine, Baylor College of Medicine, and [4]The Texas Children's Hospital, Houston; Departments of [5]Surgery (Ophthalmology), [6]Genetics, and [7]Medicine, Memorial University of Newfoundland, St. John's, Canada; [8]Ottawa Hospital Eye Institute, Ottawa, Canada; [9]Wills Eye Hospital, Philadelphia; [10]International Center for Eye Health, University College London, London; and [11]McKusick-Nathans Institute of Genetic Medicine, Johns Hopkins University, Baltimore

Some isolated populations exhibit an increased prevalence of rare recessive diseases. The island of Newfoundland is a characteristic geographic isolate, settled by a small number of families primarily during the late 1700s and early 1800s. During our studies of this population, we identified a group of families exhibiting a retinal dystrophy reminiscent of retinitis punctata albescens but with a substantially lower age at onset and more-rapid and distinctive progression, a disorder that we termed "Newfoundland rod-cone dystrophy" (NFRCD). The size of one of these families was sufficient to allow us to perform a genomewide screen to map the NFRCD locus. We detected significant linkage to markers on the long arm of chromosome 15, in a region encompassing *RLBP1*, the gene encoding the cellular retinaldehyde–binding protein. Previously, mutations in *RLBP1* have been associated with other retinal dystrophies, leading us to hypothesize that *RLBP1* mutations might also cause NFRCD. To test this hypothesis, we sequenced all coding exons and splice junctions of *RLBP1*. We detected two sequence alterations, each of which is likely to be pathogenic, since each segregates with the disease and is predicted to interfere with mRNA splicing. In contrast to some previously reported *RLBP1* mutations, which yield a protein that may retain some residual activity, each NFRCD mutation is likely to give rise to a null allele. This difference may account for the severe phenotype in these families and exemplifies the molecular continuum that underlies clinically distinct but genetically related entities.

Introduction

During phototransduction, the chromophore portion of rhodopsin, 11-*cis* retinaldehyde, is converted to all-*trans* retinaldehyde. Photoisomerized all-*trans* retinaldehyde must be recycled back into 11-*cis* retinaldehyde, in what is termed the "rod visual cycle." This process involves *RLBP1* [MIM 180090], which encodes the cellular retinaldehyde-binding protein (CRALBP) (Crabb et al. 1988; Sparkes et al. 1992; Intres et al. 1994). In the retinal pigment epithelium (RPE), CRALBP associates with the 11-*cis* retinol intermediate as well as with the regenerated 11-*cis* retinaldehyde (Saari 2000). Because of the primary function of CRALBP as an acceptor of 11-*cis* retinol during the isomerization portion of the visual cycle (Saari et al. 2001), it is not surprising that mutations in this gene have been associated with various retinal dystrophies, such as Bothnia dystrophy (BD) (Burstedt et al. 1999, 2001; Gränse et al. 2001), retinitis punctata albescens (RPA [MIM 136880]) (Morimura et al. 1999; Katsanis et al. 2001*c*), retinitis pigmentosa (RP [MIM 268000]) (Maw et al. 1997), and fundus albipunctatus (FA [MIM 136880]) (Katsanis et al. 2001*c*).

We identified six Newfoundland pedigrees with a severe rod-cone–dystrophy phenotype (NFRCD), which has an ophthalmoscopic appearance similar to that of RPA—but with age at onset typically in the 1st decade of life and with rapid progression, leading to legal blindness by the 2d–4th decades and to a further decrease in visual acuity (such that, by the 5th decade, the affected individual is, at best, only able to count fingers). We performed a genomewide screen with the largest of the six pedigrees and found statistically significant linkage to markers on the long arm of chromosome 15. Examination of the NFRCD critical interval suggested several candidate genes, among which was *RLBP1*. Because previous studies had found association with several retinal dystrophies, we hypothesized that mutations in this gene could be responsible for NFRCD, and we

Received December 13, 2001; accepted for publication January 11, 2002; electronically published February 26, 2002.

Address for correspondence and reprints: Dr. Nicholas Katsanis, McKusick-Nathans Institute of Genetic Medicine, Johns Hopkins University, 600 North Wolfe Street, Jefferson Street Building, Room 2-127, Baltimore, MD 21287. E-mail: katsanis@jhmi.edu

* The first two authors contributed equally to this work.

0002-9297/2002/7004-0013$15.00

examined our study cohort for sequence alterations in *RLBP1*. We report the identification of two splice-junction mutations that are present in different combinations in six NFRCD pedigrees and that are likely to cause disease. We also correlate the NFRCD mutations to their resulting phenotype, in the context of other *RLBP1* mutations associated with previously identified distinct clinical entities. In contrast to expected homozygosity due to a founder effect, each mutation is transmitted through two different haplotypes, suggesting that the Newfoundland population is more diverse genetically than previously postulated (Bear et al. 1988).

Subjects and Methods

Subjects

Twenty-six patients (ages 5–56 years) with a distinctive autosomal recessive retinal dystrophy most closely resembling RPA were ascertained through 12 probands referred to the Memorial University of Newfoundland Ocular Genetics Clinic. Nineteen of these patients live within a 10-mile radius in a Newfoundland area that, until recently, had remained isolated, being settled during the mid-18th century by immigrants from southwestern England. During the last century, ancestors of the two other clusters of patients migrated from this area of Newfoundland to other parts of the island.

A detailed family history was obtained from each proband, older relatives were interviewed, and archives were searched, to establish connections between different families. A single common ancestor has not been identified. However, 15 of the subjects are included in one extended pedigree, and five smaller families have 2 or 3 affected individuals each. Since several surnames recur in the earliest documentable generation, and since communities in this area existed for several generations earlier, it was originally assumed that there was a single founder mutation responsible for the disease in all these pedigrees.

Most subjects have been followed for >22 years, with ophthalmological examination, visual-field testing (Goldmann or automated perimetry), color-vision testing (Ishihara, HRR pseudoisochromatic plates, and Farnsworth D-15), dark-adaptation testing (Goldmann-Weekers adaptometer), electroretinography (ERG) (Nicolet Spirit evoked potential with gold-foil electrodes), retinal photography, and fluorescein angiography. The ERG testing included (*a*) low- and high-intensity full-field blue stimuli in dark-adapted conditions, to elicit rod responses; (*b*) maximum-intensity white stimuli, to elicit rod and cone responses; and (*c*) high-intensity white stimuli in light-adapted conditions and 30-Hz flicker stimuli, to elicit cone responses.

Blood samples were collected, and DNA was extracted from white blood lymphocytes, as described elsewhere (Katsanis et al. 2000). Selected patients had plasma ornithine levels measured, to exclude gyrate atrophy. Each patient—or, in the case of minors, parent—signed a consent statement for participation in these investigations, which were approved by the Human Investigation Committee of the Faculty of Medicine, Memorial University of Newfoundland, and the Institutional Review Board for Human Subject Research, Baylor College of Medicine.

Genotyping and Linkage Studies

A genomewide screen was performed on available DNA samples, with fluorescently tagged, published markers (ABI Prism Linkage Mapping Set-MD10 version 2; Applied Biosystems). The data were analyzed, and genotypes were deduced by the GeneScan Analysis and Genotyper software (Applied Biosystems). Linkage analysis was performed—and haplotypes were constructed—with data from both of the polymorphic markers flanking the region with *RLBP1* and with mutational data, as described elsewhere (Katsanis et al. 1999; Beales et al. 2001).

Mutation Screening

Primers were designed to amplify exons and intronic splice junctions of *RLBP1* from all available DNA samples, as well as from control samples, from Newfoundland (Katsanis et al. 2001*a;* also see the Web site of the Lupski Lab). PCR products were purified, sequenced, and analyzed as described elsewhere (Katsanis et al. 2001*a*).

Results

Clinical Evaluation

In NFRCD, night blindness is present from infancy; progressive loss of peripheral, central, and color vision begins in childhood and results in severe visual loss by the 2d–4th decade of life. Glaucoma and lens opacities have not been identified. Bone spicule pigmentation, characteristic of RP, is not seen, disks are either normal or minimally pale until a late stage, and only mild attenuation of retinal vessels is observable until the disease is advanced. In striking contrast to BD, the maculae are normal or exhibit a "beaten-bronze" atrophy.

A perimacular ring of white stippling similar to that in RPA is observed in young patients, and a scallop-bordered lacunar atrophy of the midperipheral RPE develops over time. This is similar in appearance to early gyrate atrophy or choroideremia; however, plasma ornithine levels are normal, cataracts have not been documented, and myopia is not consistently seen. Because of the common geographic origin of our subjects, the relationships established through family history and archival searches, and the opportunity that we had to examine patients over an extended period of time (up to 25 years), it became clear

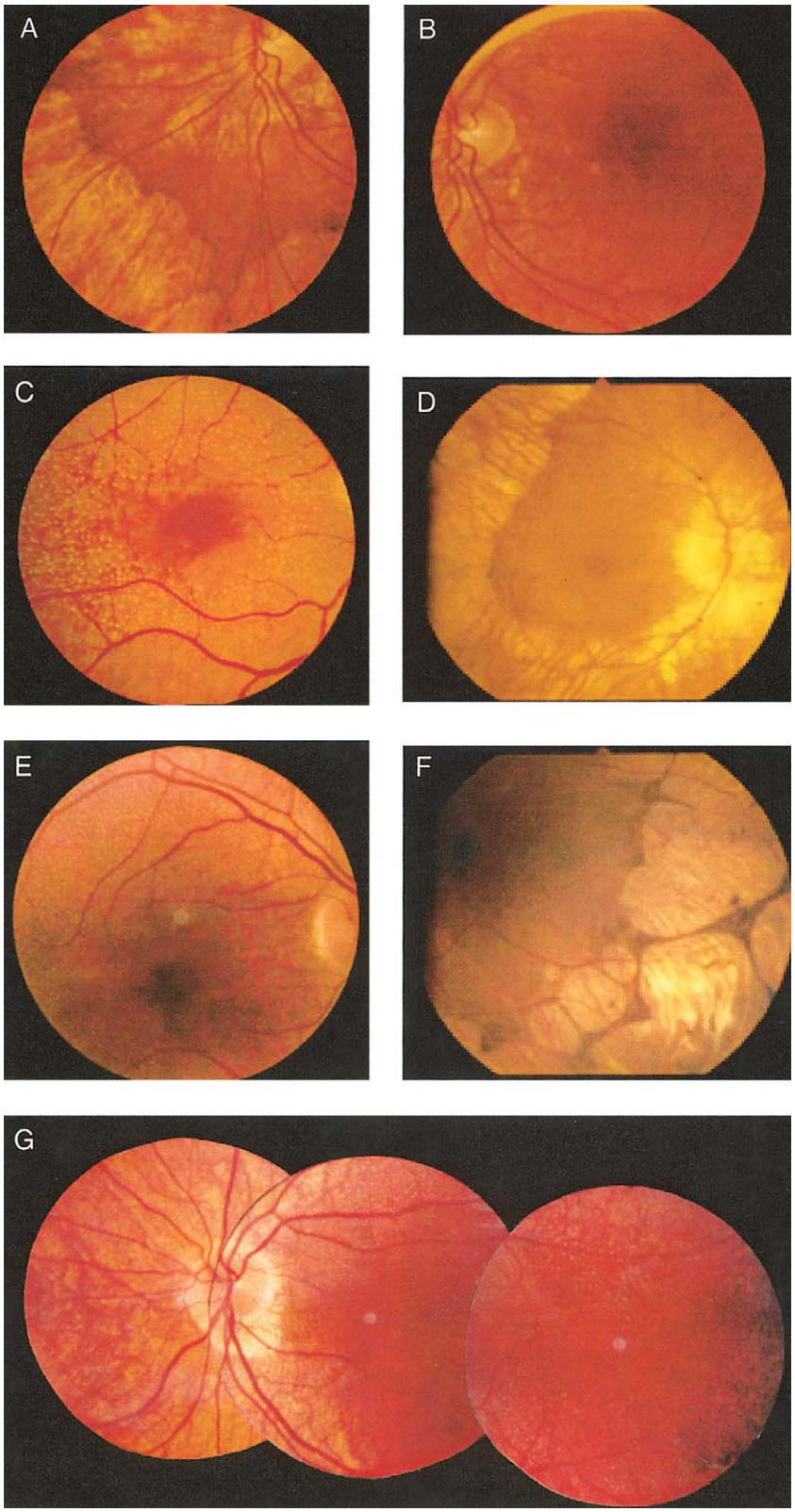

Figure 1 Fundus appearance at early, middle, and late stages of NFRCD. The left eyes of NF-001-p09, at age 54 years, exhibiting RPA and scallop-bordered atrophy inferonasally (*A* and *B*), of NF-001-p24 at age 34, with RPA (*C*), of NF-004-p02, at age 66 years, with peripheral lacunar atrophy (*D*), and of NF-001-p18, at ages 27 years (*E*) and 46 years (*F*), showing progression from RPA to advanced atrophy. Also shown is a composite of the fundus of NF-001-p18, at age 27 years (*G*).

Table 1

Clinical and Electrophysiologic Characteristics of Patients with NFRCD

Case	Age (years)		Refraction	Visual Acuity[a]	Color-Vision Defect	Visual Field[b]	Dark Adaptation [Age, in years] (log units)	ERG[c] (μv)			
	When Studied	When Blindness Was Registered						Rod	Rod/Cone	Cone	Flicker
3-p03	8	…	Plano	6/7.5; 6/12	…	Normal	…	…	…	…	…
5-p02	12	…	…	6/15; 6/18	Strong R/G	Ring scotoma 5°-25°	…	NR	<10	<10	<10
1-p01	13	…	Myopia	6/18; 6/18	Mild R/G, B/Y	Ring scotoma 10°-25°	4.5 [12]	NR	61.5	…	55
5-p01	17	…	…	6/18; 6/21	Mild R/G, B/Y	Central 10° + peripheral islands	…	NR	NR	12.5	11
3-p04	19	…	…	6/12; CF	Strong R/G	Ring scotoma 10°-25°	…	NR	28.6	14.0	NR
1-p02	23	6	High myopia	6/60; 6/90	Strong R/G, B/Y	Constricted to 10°	4.5 [10]	NR	NR	NR	NR
1-p31	25	16	Myopia	CF; CF	Strong R/G, B/Y	15° central scotoma	4 [18]	…	…	…	…
6-p01	27	20	High myopia	6/60; 6/120	…	<1° central + peripheral islands	…	NR	NR	14	10
1-p32	29	29	High myopia	HM; HM	No color perception	Ring scotoma 5°-30° at age 11	4 [11]	…	…	…	…
1-p38	32	…	Myopia	6/21; 6/21	Strong R/G, B/Y	Ring scotoma 1°-20°	4 [16]	NR	46.2	26.9	34.2
1-p45	34	34	High myopia	6/60; 6/60	Strong R/G, B/Y	Peripheral islands only	4.5 [19]	NR	19.7	19.6	12
1-p16	40	…	Plano	6/6; 6/6	Mild R/G	Ring scotoma 3°-30°	4.5 [33]	NR	NR	27.3	28.9
1-p44	40	40	High myopia	HM; 6/60	Strong R/G, B/Y	Ring scotoma 5°-25° (G III 4)	…	NR	22.7	18.6	16.8
8-p02	40	…	High myopia	6/120; 6/9	No color perception	Central scotoma + peripheral constriction	…	…	…	…	…
1-p47	45	…	Hyperopia	6/9; 6/9	Strong R/G, B/Y	…	4.5 [32]	…	…	…	…
1-p18	46	46	Plano	6/60; 6/18	Moderate R/G, B/Y	Peripheral islands only	4.5 [33]	NR	NR	11.3	NR
6-p03	48	35	Hyperopia	CF; CF	…	…	…	…	…	…	…
1-p24	49	…	Hyperopia	6/60; 6/30	Strong R/G, B/Y	Ring scotoma 1°-30°	4.5 [34]	NR	NR	50.7	35.9
1-p39	50	31	Hyperopia	6/120; 6/120	Strong R/G, B/Y	Peripheral islands only	4.5 [35]	NR	NR	NR	NR
8-p01	52	45	Plano	6/120; 6/120	Strong R/G, B/Y	Peripheral islands only	…	NR	NR	NR	NR
4-p01	55	<55	Myopia	HM; HM	…	Peripheral islands only (G V 4)	…	…	…	…	…
3-p05	56	31	Hyperopia	HM; HM	…	Peripheral islands only (G V 4)	5 [56]	NR	NR	NR	NR
1-p09	58	51	Myopia	CF; CF	Strong R/G, B/Y	Central 10° + peripheral islands	4.5 [54]	NR	NR	NR	NR
6-p02	62	24	…	PL; PL	…	No response	…	…	…	…	…
4-p03	63	51	Plano	CF; CF	Strong R/G, B/Y	Central + superior scotoma (G III 4)	4 [48]	NR	…	15	7.1
4-p02	66	53	High myopia	6/90; 6/120	Strong R/G, B/Y	Peripheral islands only	…	NR	NR	NR	NR

Note.—Ellipses (…) denote that data were not available.

[a] CF = counting of fingers; HM = hand motions; PL = perception of light.

[b] G III 4 and G IV 4 = object size (in terms of Goldmann perimeter).

[c] NR = no response.

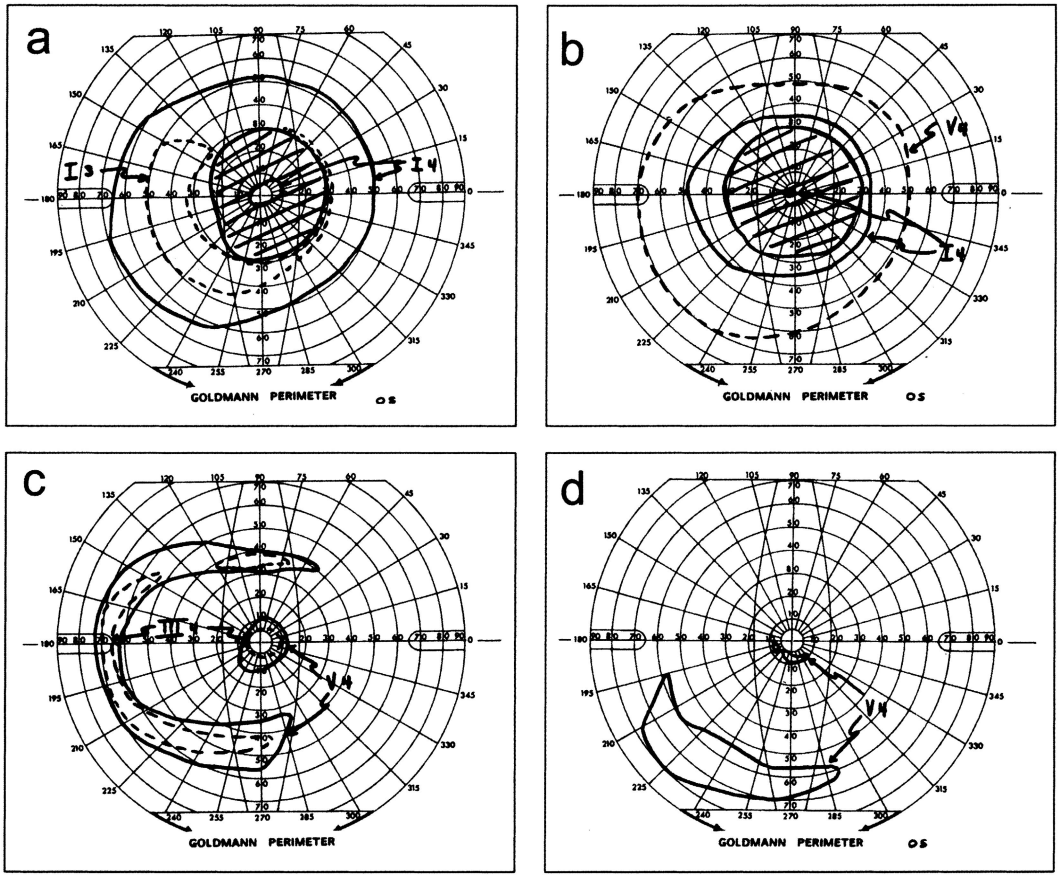

Figure 2 Visual-field defects in NFRCD with Goldmann perimeter: NF-001-p16, at age 26 years, with visual acuity 6/6, showing ring scotoma at 6–25 degrees (*a*), NF-001-p24, at age 34 years, with visual acuity 6/15, ring scotoma at 1–30 degrees (*b*), NF-001-p09, at age 54 years, with visual acuity 6/60, showing the central 10 degrees and peripheral islands only (*c*), and NF-004-p01, at age 57 years, with visual acuity restricted to detection of hand motion, peripheral islands only (*d*).

that the different retinal appearances were part of a continuum of a single disease process (fig. 1 and table 1).

The ERG rod responses are selectively reduced early, and the ERG rod and cone responses are both extinguished in advanced disease. Two young patients had a negative photopic B-wave response at first ERG test but later had significantly delayed and reduced responses to photopic white and flicker stimuli. When tested, dark adaptation thresholds during the teen years were typically raised 4–4.5 log units. In most subjects, the early visual-field defect is a ring scotoma close to fixation (fig. 2)—rather than in the midperipheral field, as in classic RP. Central visual acuity may be good (e.g., 6/6–6/21), although the central field may be only 1°–3°. The rate at which the ring scotoma widens and becomes a complete central scotoma determines the age at registration of blindness and is an indicator of the rate of progression of the disease, which may otherwise appear to be arrested.

Color-vision defects are initially mild red/green (R/G) or mild R/G and blue/yellow (B/Y) defects, but these progress rapidly to severe R/G and B/Y defects, by the 20s, and to eventual loss of color perception; however, there are exceptions in which patients in their 30s or 40s have only mild-to-moderate color-vision defects recorded. A summary of ophthalmic findings is provided in table 1.

Genotyping and Linkage Studies

We performed a genomewide screen with kindred NF-001 (fig. 3). After evaluating 285/385 markers (74% of the genome), we detected a LOD score of 5.80, at recombination fraction (θ) 0.001, with microsatellite *D15S127*. The next-closest marker tested, *D15S205,* 7.9 cM proximal to *D15S127,* also provided a positive, although not statistically significant, LOD score of 2.44 at $\theta = 0.10$, suggesting that NFRCD likely maps to 15q26, close to *D15S127*. Haplotype analysis of all available family members of NF-001 indicated that NFRCD maps distal to *D15S205,* on the basis of a re-

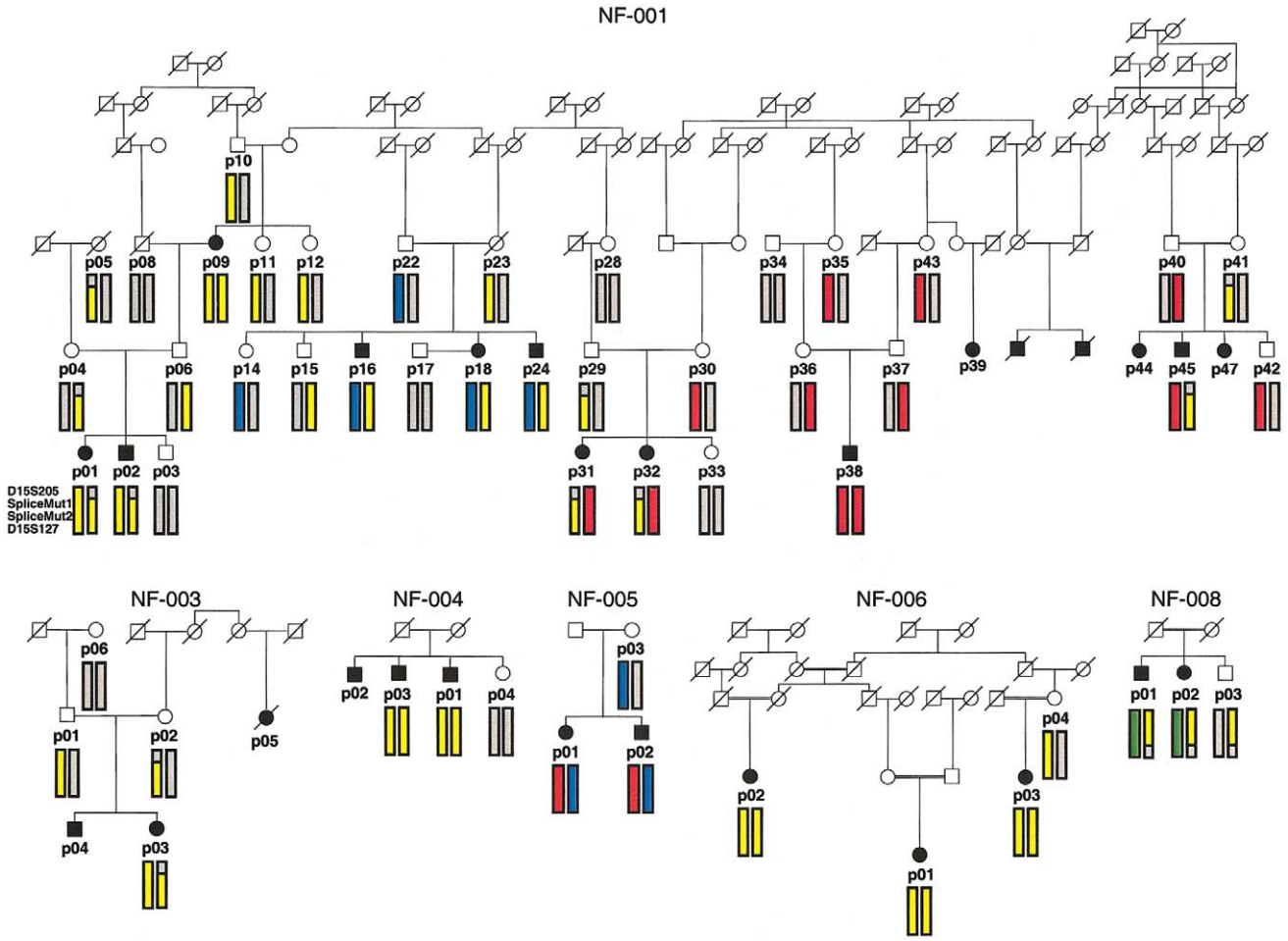

Figure 3 Mutation and haplotype data for six Newfoundland pedigrees diagnosed with NFRCD. All individuals were genotyped for *D15S205* and *D15S127* and were sequenced for *RLBP1*. Haplotypes were then constructed for *D15S205*-SpliceMut1-SpliceMut2-*D15S127*, with polymorphic alleles expressed in terms of base pairs. SpliceMut1 = 324G→A; SpliceMut2 = IVS3+2 T→C. Each colored bar represents a unique haplotype: yellow = 135-324G→A-wt-142; blue = 124-324G→A-wt-134; red = 159-wt-IVS3+2 T→C-136; green = 135-wt-IVS3+2 T→C-140; gray = non–disease-associated haplotypes.

combination, between *D15S205* and *D15S127*, that is apparent in individual p01 (fig. 3). Given that the peak LOD score for *D15S205* was at $\theta = 0.10$ and that *D15S127* is almost 8 cM away, we examined the genomic sequence between these loci for candidate genes.

RLBP1 maps within the 2-cM region of interest surrounding *D15S127*. Mutations in *RLBP1* have been implicated previously in several retinal dystrophies that share some features with the NFRCD phenotype (table 2). We thus sequenced the seven coding exons of *RLBP1*, including splice junctions, in affected individuals from NF-001. We identified two alterations that were likely pathogenic (fig. 4*A*). The first alteration was a G→A transition (324G→A) in the last base of exon 3. The second alteration was a T→C transition in the second base of intron 3 (IVS3+2 T→C). Both alterations are likely to interfere with splicing of the *RLBP1* RNA. The last base of an exon is a guanine in 73% of known genes (Mount 1982) but is an adenine in only 9%, whereas the second base of the intron is almost always a thymine (Mount 1982; Zhang 1998).

We investigated each alteration for a potential pathogenic effect. First, we sequenced all the family members of NF-001 and segregated the two alterations in the pedigree (fig. 3). All affected individuals—but none of the unaffected parents or siblings—either were homozygous for one alteration or the other or were compound heterozygotes for both (fig. 4*B*). Furthermore, the IVS3+2 T→C alteration was not found in 106 control chromosomes from Newfoundland; in one control individual, 324G→A was found in the heterozygous state, which may reflect a higher carrier frequency of this allele in Newfoundland. Third, analysis by the Delila program (see the Delila Server Entry Page), an information-based theory

Table 2

Phenotypic Spectrum of *RLBP1* Mutations

Mutation 1	Mutation 2	Phenotype(s)	Reference(s)
R150Q	R150Q	FA, RPA, RP	Maw et al. (1997); Katsanis et al. (2001*c*)
R233W	R233W	BD, RPA	Burstedt et al. (1999, 2001); Morimura et al. (1999); Gränse et al. (2001)
9483delC	9483delC	RPA	Morimura et al. (1999)
M225K	IVS3+2 T→C	RPA	Morimura et al. (1999)
IVS3+2 T→C	IVS3+2 T→C	NFRCD	Present study
IVS3+2 T→C	324G→A	NFRCD	Present study
324G→A	324G→A	NFRCD	Present study

model of donor and acceptor splice sites, assigned a bit value as a representation of the strength of interaction between the splice site and the spliceosome, for both the wild-type and the mutant splice sites (Rogan and Schneider 1995; Rogan et al. 1998). The results suggest that each of these mutations unmasks a cryptic splice site (of 5.1 bits) that is 5 bases into intron 3 and that competes with the normal splice site (for 324G→A, the bit value drops from 10.4 to 7.4 bits; for IVS3+2 T→C, the bit value drops from 10.4 to 3.0 bits). By conceptual translation, abnormal splicing will cause a frameshift that leads to premature termination early in exon 4 (fig. 4*A*), if the mRNA is not degraded. Finally, previous studies have shown that IVS3+2 T→C causes RPA in a compound heterozygote carrying a second, missense mutation, resulting in a methionine-to-lysine change (M225K) (Morimura et al. 1999). We therefore concluded that these alterations likely represent disease-associated mutations and are not benign polymorphisms.

To evaluate further the potential involvement of *RLBP1* in NFRCD, we sequenced DNA from individuals in five smaller NFRCD pedigrees; ancestors of all six pedigrees came from a defined area within a 10-mile radius. Although we anticipated a potential founder effect in Newfoundland, we could not identify a single common ancestor through archived genealogical information. The patients in NF-003, NF-004, and NF-006 were homozygous for 324G→A. In NF-005 and NF-008, both affected individuals were compound heterozygotes for the two alterations seen to segregate with the disease in NF-001 (figs. 3 and 4*B*). These data are consistent with the predicted inheritance of disease chromosomes, as determined by haplotype analysis, and further substantiate the hypothesis that *RLBP1* dysfunction is responsible for the NFRCD phenotype.

Discussion

We have reported a distinct rod-cone dystrophy phenotype, NFRCD, in six Newfoundland families that may be unique to that geographic area. We have detected linkage of NFRCD to a chromosome 15q26 region encompassing *RLBP1,* a gene that previously has been associated with several disorders of the retina. Sequencing of exons and splice junctions has revealed two pathogenic alterations that segregate with the disease in all pedigrees with NFRCD and that are predicted to interfere with mRNA processing, suggesting that *RLBP1* dysfunction is responsible for this disorder.

NFRCD is the first instance in which patients inherit two *RLBP1* splice-junction mutations (table 2). Thus far, primarily missense mutations have been identified in *RLBP1.* A homozygous missense mutation in exon 7, 9096C→T, which causes a R233W substitution, has been associated with both BD (Burstedt et al. 1999, 2001; Gränse et al. 2001) and RPA (Morimura et al. 1999). Also, autosomal recessive RP has been associated with a homozygous missense mutation in exon 5, 4763G→A, which causes an R150Q change (Maw et al. 1997). This same mutation also has been described in a pedigree diagnosed with FA and RPA, depending on the patients' age at evaluation (Katsanis et al. 2001*c*). Finally, RPA has been reported both in one patient with a homozygous 1-bp deletion (9483delC) in exon 8 and in a patient who is a compound heterozygote with a splice-donor mutation in intron 3 (IVS3+2 T→C) and a missense mutation in exon 6 (M225K) (Morimura et al. 1999).

The clinical distinction between FA, RP, and RPA may be subtle and dependent on the age at diagnosis. For instance, a long-term study of a pedigree with a R150Q mutation revealed that patients could be diagnosed either with FA, during the 2d decade of life, or with RPA, during the 4th and 5th decade (Katsanis et al. 2001*c*). Therefore, although NFRCD appears to manifest early and exhibits a rapid progression and substantial or total loss of vision by the 4th or 5th decade of life, distinctions based on age at onset are not reliable, both because of subjective ascertainment bias and because of substantial inter- and intrafamilial variability. The lack of macular involvement may potentially be a feature that distinguishes between NFRCD and BD.

Likewise, genotype-phenotype correlations in these retinal dystrophies may be difficult to detect (table 1; also see Burstedt et al. 2001). Newfoundland-specific variation in other genes may contribute to the severity

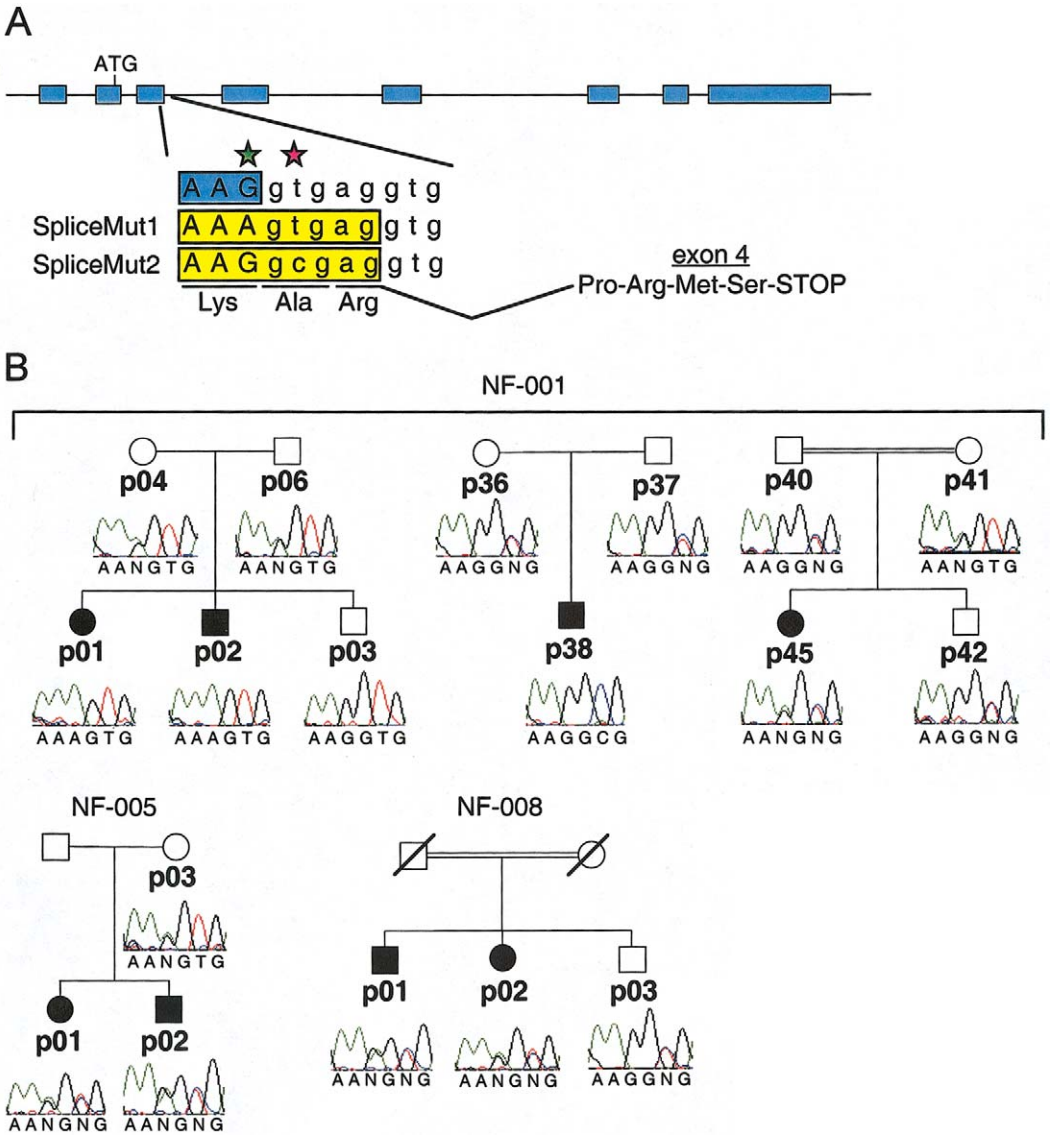

Figure 4 Location of mutations in *RLBP1*, and pedigrees harboring the mutations. *A*, Two splice mutations observed at the exon 3/intron 3 junction and predicted to activate a cryptic splice site 6 bp into intron 3. This splice site will create a transcript that, if translated, will produce a protein that terminates early in exon 4. SpliceMut1 = 324G→A; SpliceMut2 = IVS3+2 T→C. *B*, Subsets of the large pedigree NF-001 and of pedigrees NF-005 and NF-008. Patients NF-001-p01 and NF-001-p02 are homozygous for the 324G→A mutation. NF-001-p38 is homozygous for the IVS3+2 T→C mutation, whereas NF-001-p45 is heterozygous for each mutation. Patients in NF-005 and NF-008 are heterozygous for both alterations.

of the phenotype of patients with NFRCD patients and to clinically related entities such as BD and RPA. This variation is not likely, however, since the RPA phenotype—but not the more severe NFRCD phenotype—has been reported in different populations, including Swedes from the Gulf of Bothnia, Saudi Arabians, Indians, and white Europeans of various backgrounds. More important, if the severity of the disease reflects variation at other loci, then we might expect that milder, RPA-like phenotypes would also be prevalent in Newfoundland, which is not the case.

The clinical stratification of *RLBP1*-based mutations is more likely to depend on the effect that the mutations have on the protein and the cell. The impact that the splice-junction mutations have on the mRNA is difficult to assess directly. *RLBP1* expression is restricted to the retinal Müller cells, pineal gland, RPE, iris, cornea, and oligodendrocytes of the optic nerve and brain (Bunt-Milam and Saari 1983; Bridges et al. 1987; Saari et al. 1997) and is not present in peripheral-blood cells or lymphocytes, and retinas from affected individuals are not available. Nevertheless, each splice-junction muta-

tion is predicted to activate a cryptic splice site in intron 3; conceptually, this activation would result in either a truncated protein product (fig. 4*A*) or, more likely, degradation of the incorrectly spliced transcript via nonsense-mediated RNA decay (reviewed in Culbertson 1999; Frischmeyer and Dietz 1999; Hentze and Kulozik 1999). By contrast, missense *RLBP1* mutations may compromise the function of the protein, but are not likely to impact the message. The reported 1-bp deletion lies in the last exon and thus is not subject to RNA decay (Maquat 2000; Lykke-Andersen 2001); an extended protein is the expected outcome (Morimura et al. 1999).

Comparison of the haplotypes of the disease-carrying chromosomes in the six pedigrees also reveals two distinct haplotypes associated with the 324G→A mutation and two haplotypes associated with the IVS3+2 T→C mutation (fig. 3). These data suggest either that both mutations were introduced into Newfoundland through two independent mutation events on two different chromosomes or that each mutation is relatively old and has undergone haplotype divergence. Furthermore, the higher prevalence of the 324G→A mutation suggests that this might be the initial mutation introduced into that population, a hypothesis consistent with the presence of this mutation in 1/106 Newfoundland control chromosomes and in 0/112 non-Newfoundland control chromosomes.

These observations, coupled with the presence of two distinct mutations within the same pedigree, suggest that genetic homogeneity in the island of Newfoundland may be less than what would be expected on the basis of historical and genealogical data. This inference is consistent with data from other recessive disorders commonly found in this geographic region. Recent studies have identified four distinct Newfoundland mutations in *BBS6,* one of the genes causing Bardet-Biedl syndrome (BBS), as well as two distinct disease-associated haplotypes for the uncloned *BBS1* locus, in what has been termed "the Newfoundland paradox" (Katsanis et al. 2000, 2001*b;* Beales et al. 2001). For BBS, this phenomenon is even more pronounced, since one Newfoundland pedigree also has been shown to require two recessive mutations at one BBS locus (i.e., *BBS2*), coupled with a single mutation at a second BBS locus (i.e., *BBS6*), for the phenotype to manifest (Katsanis et al. 2001*a*).

Finally, we note that individual NF-001-p45 and both affected individuals in pedigree NF-008 are the offspring of consanguineous matings, for which we might expect a homozygous *RLBP1* mutation as well as identity by descent (IBD) for markers near the locus. These individuals, however, are heterozygous both for each of the Newfoundland mutations and for the markers spanning the critical interval (figs. 3 and 4*B*). Therefore, IBD-based genetic screening, a common and often successful practice in the genetic analysis of population isolates, would likely miss this locus. Alternative inheritance hypotheses must therefore be considered even in population isolates, since genetic homogeneity may be overestimated.

Acknowledgments

We thank the families for their willing and continued participation. We thank Dr. Richard Alan Lewis for his critical evaluation of the manuscript, and we thank Dr. Thomas D. Schneider for his assistance in splice-site analysis. This study was supported in part by National Eye Institute (National Institutes of Health) grant EY12666 (to N.K.) and by the March of Dimes (support to N.K. and J.R.L.), the Foundation Fighting Blindness, USA (support to J.R.L.), the Kleberg Foundation (support to D.W.S.), the Kidney Foundation of Canada (support to J.S.G.), the Janeway Foundation (support to J.S.G.), the Canadian Institutes of Health Research (support to J.S.G. and G.J.J.), and the Foundation Fighting Blindness, Canada (support to J.S.G. and G.J.J.).

Electronic-Database Information

Accession numbers and URLs for data in this article are as follows:

Delila Server Entry Page, http://www.lecb.ncifcrf.gov/~toms/delilaserver.html

Lupski Lab home page, http://www.imgen.bcm.tmc.edu/molgen/lupski/index.html

Online Mendelian Inheritance in Man (OMIM), http://www.ncbi.nlm.nih.gov/Omim (for RLBP1 [MIM 180090], RPA/FA [MIM 136880], and RP [MIM 268000])

References

Beales PL, Katsanis N, Lewis RA, Ansley SJ, Raza J, Woods MO, Green JS, Parfrey PS, Davidson WS, Lupski JR (2001) Genetic and mutational analyses of a large multi-ethnic Bardet-Biedl cohort reveal a minor involvement of *BBS6* and delineate the critical intervals of other loci. Am J Hum Genet 68:606–616

Bear JC, Nemec TF, Kennedy JC, Marshall WH, Power AA, Kolonel VM, Burke GB (1988) Inbreeding in outport Newfoundland. Am J Med Genet 29:649–660

Bridges CD, Foster RG, Landers RA, Fong SL (1987) Interstitial retinol-binding protein and cellular retinal-binding protein in the mammalian pineal. Vision Res 27:2049–2060

Bunt-Milam AH, Saari JC (1983) Immunocytochemical localization of two retinoid-binding proteins in vertebrate retina. J Cell Biol 97:703–712

Burstedt MS, Forsman-Semb K, Golovleva I, Janunger T, Wachtmeister L, Sandgren O (2001) Ocular phenotype of Bothnia dystrophy, an autosomal recessive retinitis pigmentosa associated with an R234W mutation in the *RLBP1* gene. Arch Ophthalmol 119:260–267

Burstedt MS, Sandgren O, Holmgren G, Forsman-Semb K

(1999) Bothnia dystrophy caused by mutations in the cellular retinaldehyde-biding protein gene (*RLBP1*) on chromosome 15q26. Invest Ophthalmol Vis Sci 40:995–1000

Crabb JW, Goldflam S, Harris SE, Saari JC (1988) Cloning of the cDNAs encoding the cellular retinaldehyde-binding protein from bovine and human retina and comparison of the protein structures. J Biol Chem 263:18688–18692

Culbertson MR (1999) RNA surveillance: unforeseen consequences for gene expression, inherited genetic disorders and cancer. Trends Genet 15:74–80

Frischmeyer PA, Dietz HC (1999) Nonsense-mediated mRNA decay in health and disease. Hum Mol Genet 8:1893–1900

Gränse L, Abrahamson M, Ponjavic V, Andréasson S (2001) Electrophysiological finding in two young patients with Bothnia dystrophy and a mutation in the RLBP1 gene. Ophthalmic Genet 22:97–105

Hentze MW, Kulozik AE (1999) A perfect message: RNA surveillance and nonsense-mediated decay. Cell 96:307–310

Intres R, Goldflam S, Cook JR, Crabb JW (1994) Molecular cloning and structural analysis of the human gene encoding cellular retinaldehyde-binding protein. J Biol Chem 269: 25411–25418

Katsanis N, Ansley SJ, Badano JL, Eichers ER, Lewis RA, Hoskins BE, Scambler PJ, Davidson WS, Beales PL, Lupski JR (2001*a*) Triallelic inheritance in Bardet-Biedl syndrome, a Mendelian recessive disorder. Science 293:2256–2259

Katsanis N, Beales PL, Woods MO, Lewis RA, Green JS, Parfrey PS, Ansley SJ, Davidson WS, Lupski JR (2000) Mutations in *MKKS* cause obesity, retinal dystrophy and renal malformations associated with Bardet-Biedl syndrome. Nat Genet 26:67–70

Katsanis N, Lewis RA, Stockton DW, Mai PMT, Baird L, Beales PL, Leppert M, Lupski JR (1999) Delineation of the critical interval of Bardet-Biedl syndrome 1 (*BBS1*) to a small region of 11q13, through linkage and haplotype analysis of 91 pedigrees. Am J Hum Genet 65:1672–1679

Katsanis N, Lupski JR, Beales PL (2001*b*) Exploring the molecular basis of Bardet-Biedl syndrome. Hum Mol Genet 10: 2293–2299

Katsanis N, Shroyer NF, Lewis RA, Cavender JC, Al-Rajhi AA, Jabak M, Lupski JR (2001*c*) Fundus albipunctatus and retinitis punctata albescens in a pedigree with an R150Q mutation in *RLBP1*. Clin Genet 59:424–429

Lykke-Andersen J (2001) mRNA quality control: marking the message for life or death. Curr Biol 11:R88–R91

Maquat LE (2000) Nonsense-mediated RNA decay in mammalian cells: a splicing-dependent means to down-regulate the levels of mRNAs that prematurely terminate translation. In: Hershey JWB, Mathews MB, Sonenberg N (eds) Translational control. Cold Spring Harbor Press, Cold Spring Harbor, NY, pp 827–868

Maw MA, Kennedy B, Knight A, Bridges R, Roth KE, Mani EJ, Mukkadan, JK, Nancarrow D, Crabb JW, Denton MJ (1997) Mutation of the gene encoding cellular retinaldehyde-binding protein in autosomal recessive retinitis pigmentosa. Nat Genet 17:198–200

Morimura H, Berson EL, Dryja TP (1999) Recessive mutations in the *RLBP1* gene encoding cellular retinaldehyde-binding protein in a form of retinitis punctata albescens. Invest Ophthalmol Vis Sci 40:1000–1004

Mount S (1982) A catalogue of splice junction sequences. Nucleic Acids Res 10:459–472

Rogan PK, Faux BM, Schneider TD (1998) Information analysis of human splice site mutations. Hum Mutat 12:153–171

Rogan PK, Schneider TD (1995) Using information content and base frequencies to distinguish mutations from genetic polymorphisms in splice junction recognition sites. Hum Mutat 6:74–76

Saari JC (2000) Biochemistry of visual pigment regeneration: The Friedenwald Lecture. Invest Ophthalmol Vis Sci 41: 337–348

Saari JC, Huang J, Possin DE, Fariss RN, Leonard J, Garwin GG, Crabb JW, Milam AH (1997) Cellular retinaldehyde-binding protein is expressed by oligodendrocytes in optic nerve and brain. Glia 21:259–268

Saari JC, Nawrot M, Kennedy BN, Garwin GG, Hurley JB, Huang J, Possin DE, Crabb JW (2001) Visual cycle impairment in cellular retinaldehyde binding protein (CRALBP) knockout mice results in delayed dark adaptation. Neuron 29:739–748

Sparkes RS, Heinzmann C, Goldflam S, Kojis T, Saari JC, Mohandas T, Klisak I, Bateman JB, Crabb JW (1992) Assignment of the gene (RLBP1) for cellular retinaldehyde-binding protein (CRALBP) to human chromosome 15q26 and mouse chromosome 7. Genomics 12:58–62

Zhang MQ (1998) Statistical features of human exons and their flanking regions. Hum Mol Genet 7:919–932